The Company of **Biologists**

RESEARCH ARTICLE

Transcriptional induction of cell wall remodelling genes is coupled to microtubule-driven growth isotropy at the shoot apex in *Arabidopsis*

Alessia Armezzani[1], Ursula Abad[1], Olivier Ali[1,2], Amélie Andres Robin[1], Laetitia Vachez[1], Antoine Larrieu[1,*], Ewa J. Mellerowicz[3], Ludivine Taconnat[4,5], Virginie Battu[1], Thomas Stanislas[1], Mengying Liu[1], Teva Vernoux[1], Jan Traas[1,‡] and Massimiliano Sassi[1]

ABSTRACT

The shoot apical meristem of higher plants continuously generates new tissues and organs through complex changes in growth rates and directions of its individual cells. Cell growth, which is driven by turgor pressure, largely depends on the cell walls, which allow cell expansion through synthesis and structural changes. A previous study revealed a major contribution of wall isotropy in organ emergence, through the disorganization of cortical microtubules. We show here that this disorganization is coupled with the transcriptional control of genes involved in wall remodelling. Some of these genes are induced when microtubules are disorganized and cells shift to isotropic growth. Mechanical modelling shows that this coupling has the potential to compensate for reduced cell expansion rates induced by the shift to isotropic growth. Reciprocally, cell wall loosening induced by different treatments or altered cell wall composition promotes a disruption of microtubule alignment. Our data thus indicate the existence of a regulatory module activated during organ outgrowth, linking microtubule arrangements to cell wall remodelling.

KEY WORDS: Auxin, Cell wall, Microtubules, Morphogenesis, Shoot apical meristem

INTRODUCTION

The control of shape during growth of multicellular organisms is a fundamental, yet poorly understood, process. In the animal field, major efforts have been focused on how cell migration, rapid changes in cell shape and apoptosis contribute to morphogenesis (see Gilmour et al., 2017 for a review). By contrast, the processes related to growth have received most of the attention in plants, which represent an excellent model in which to investigate this aspect (Coen et al., 2004; Sassi and Traas, 2015; Traas and Hamant, 2009).

[1]Laboratoire de Reproduction et Développement des Plantes, Universite de Lyon, ENS de Lyon, UCBL, INRA, CNRS, 46 Allée d'Italie, 69364 Lyon Cedex 07, France. [2]INRIA team MOSAIC, Laboratoire de Reproduction et Développement des Plantes, Université de Lyon, ENS de Lyon, INRA, CNRS, 46 Allée d'Italie, 69364 Lyon Cedex 07, France. [3]Department of Forest Genetics and Plant Physiology, Swedish University of Agricultural Sciences (Sveriges lantbruksuniversitet), S901-83 Umea, Sweden. [4]Institute of Plant Sciences Paris Saclay IPS2, CNRS, INRA, Université Paris-Sud, Université Evry, Université Paris-Saclay, Bâtiment 630, 91405 Orsay, France. [5]Institute of Plant Sciences Paris-Saclay IPS2, Paris Diderot, Sorbonne Paris-Cité, Bâtiment 630, 91405 Orsay, France.
*Present address: Faculty of Biological Sciences, University of Leeds, Leeds LS2 9JT, UK.

‡Authors for correspondence (jan.traas@ens-lyon.fr)

A.A., 0000-0002-5816-402X; J.T., 0000-0001-5107-1472; M.S., 0000-0002-9685-4902

Indeed, in contrast to their animal counterparts, plant cells usually do not migrate or rapidly change shape during development, while programmed cell death does not, in principle, play an important role. As a result, morphogenesis in plants is entirely determined by local growth rates and growth directions.

Plant growth depends largely on the dynamics of the extracellular matrix or cell wall, which surrounds most cells and counteracts the high internal turgor pressure. In higher plants, this wall is largely composed of relatively stiff cellulose microfibrils that are cross-linked by a matrix of polysaccharides such as hemicelluloses, pectins and structural proteins (for reviews, see Park and Cosgrove, 2012b; Cosgrove, 2016b; Traas and Hamant, 2009; Braybrook and Jönsson, 2016). In order to grow, cells have to expand their cell walls irreversibly, making them yield to the internal pressure. It is therefore thought that molecular regulation largely controls morphogenesis by affecting the local biochemical composition and arrangements of the cell wall polysaccharides.

A plethora of cell wall remodelling and synthesizing proteins have been identified. The precise number of synthesizing proteins is not known, but it is thought that hundreds of enzymes may be involved in this process (e.g. Yang et al., 2016). In addition, several multigene families encode proteins that are likely involved in modifying the existing bonds, potentially affecting the mechanical properties of the wall, although their precise function is still a matter of debate (Cosgrove, 2016a,b). The best known of these so-called remodelling proteins include: (1) the pectin methyl esterase (PME) family and their inhibitors (PMEIs), which control the assembly and mechanical properties of the pectin matrix (Levesque-Tremblay et al., 2015); (2) the xyloglucan endo-transglucosylase/hydrolase (XTH) family (Nishitani, 2006; Rose et al., 2002), which is supposed to act on the mechanical properties of the hemicellulose matrix; and (3) the A-type expansin (EXPA) family, which supposedly interferes with wall assembly and maybe also wall mechanics. [EXPAs might interfere with the interactions between hemicellulose and cellulose (Cosgrove, 2015).]

The remodelling of pectin and hemicellulose polysaccharides has the potential to modulate overall growth rates. Although matrix polymers have also been associated with the control of growth anisotropy (Peaucelle et al., 2015), growth directions in many tissues are largely determined by the presence of cellulose microfibril arrays in the cell wall. The polymers can be deposited in highly ordered arrays, restricting cell expansion along their axis. The orientation of the cellulose microfibrils themselves is controlled by cortical microtubules (CMTs), which guide the movement of the cellulose synthase (CESA) complexes across the plasma membranes (Paredez et al., 2006). Although the exact mechanism underlying microtubule orientation is not known, several components of the Rho proteins

DEVELOPMENT

1

of plants (ROP) signalling pathway seem to be involved. Indeed, mutations in ROP6 and ROP INTERACTING PROTEIN AND CRIB MOTIF-CONTAINING PROTEIN 1 (RIC1) affect microtubule organization at the shoot apex, and influence organ formation (Sassi et al., 2014). RIC1 itself directly interacts with BOTERO1/KATANIN (BOT1/KTN), a microtubule-associated protein required for microtubule severing and bundling (Lin et al., 2013). Consistently, mutations in BOT1/KTN (hereinafter *bot1*) also affect meristem function (Sassi et al., 2014).

In summary, to control growth directions and growth rates at the level of the cell wall, the regulatory molecular networks can act on two sets of parameters: (1) the composition and the structure of the wall; and (2) the orientation of the cellulose microfibrils, in particular via microtubule dynamics. However, the coordination of these parameters and their relative contributions to morphogenesis are not understood.

The shoot apical meristem (SAM) of *Arabidopsis thaliana* represents an ideal system for addressing these issues. As it harbours the stem cells, the SAM continuously generates new tissues and organs at the shoot tip, which involves complex changes in cell growth directions and in cell growth rates (Sassi et al., 2014; Kwiatkowska, 2004; Kwiatkowska and Dumais, 2003). Organ formation at the SAM is initiated by the accumulation of the hormone auxin in discrete *foci* at the periphery of the meristem (Reinhardt et al., 2000; Reinhardt et al., 2003). This is achieved by an active transport mechanism relying on the action of the PIN-FORMED 1 (PIN1) efflux carrier.

Several studies have suggested an important role for wall remodelling during morphogenesis at the meristem. The local application of expansins can induce organ formation (Fleming et al., 1997), whereas induced changes in the degree of pectin methylation can induce or inhibit organogenesis (Peaucelle et al., 2011a). The *xxt1 xxt2* mutant, which has greatly reduced levels of the hemicellulose xyloglucan, shows abnormal plant architecture (Park and Cosgrove, 2012a; Cavalier et al., 2008). It remains nevertheless unclear how wall composition is regulated during organ formation.

In a recent study, we have shown that high auxin concentrations at organ *initia* cause the disorganization of microtubules and we proposed that a shift to isotropic growth, through the isotropic deposition of microfibrils, plays a major role in organ formation (Sassi et al., 2014). This shift could act in synergy with relatively modest changes in wall stiffness observed during organ formation. Although both wall loosening and wall isotropy seem to be involved, their relative importance and their coordination during organogenesis remain ill defined.

To address this issue, we have investigated the roles of microtubule organization and wall remodelling during morphogenesis at the SAM. For this purpose we identified genes encoding XTHs, EXPAs, PMEs and PMEIs strongly expressed at the shoot meristem. Some of these are strongly correlated with organ initiation. We provide evidence that the transcription of the genes can be activated through changes in microtubule organization, independently from auxin accumulation and transport. Conversely, interfering with wall loosening promotes changes in microtubule organization. We propose that this tight coupling between cytoskeleton organization and cell wall remodelling plays a central role in coordinating growth during organ initiation at the SAM.

RESULTS

Disorganizing the cortical microtubules increases growth rates *in vivo* but not *in silico*

To bulge out, cells in a primordium must initially grow more rapidly than the surrounding cells, in particular the boundary cells (Kwiatkowska, 2004). The partial restoration of organ outgrowth observed in the *pin1-6 bot1-7* double mutant (Sassi et al., 2014) (Fig. 1) suggests that disorganized CMTs are sufficient to cause this increase in growth rates. This is in line with the observation that the local disorganization of microtubules using the drug oryzalin (ORY) also causes the induction of local outgrowths when auxin transport is impaired (Sassi et al., 2014).

If we accept that the disorganization of microtubules primarily affects cellulose deposition, a shift to the isotropic distribution of microfibrils should then also lead to outgrowth and to an overall increase in growth rates. This leads to the somewhat counterintuitive hypothesis that not only the density of microfibrils, but also their orientation, has the potential to affect global growth rates. In other words, the experimental results indicate that, at identical microfibril density, cells with an isotropic wall would grow faster than cells with anisotropic walls. An explanation for this could be that isotropically organized microfibrils resist stress coming from all directions, but with a lower magnitude than if they were preferentially aligned in one orientation.

To further explore this hypothesis, we performed mechanical simulations of a growing meristematic dome (Fig. 2). These simulations were conducted with a dedicated numerical framework, where specific values of the mechanical wall parameters (stiffness, wall synthesis rates and yielding thresholds) and turgor pressure can be set in each cell (Boudon et al., 2015). The framework does not allow for the modelling of cell division and cannot be used for important changes in shape. Based on several observations (see, for example, Kierzkowski et al., 2012; Hacham et al., 2011), we
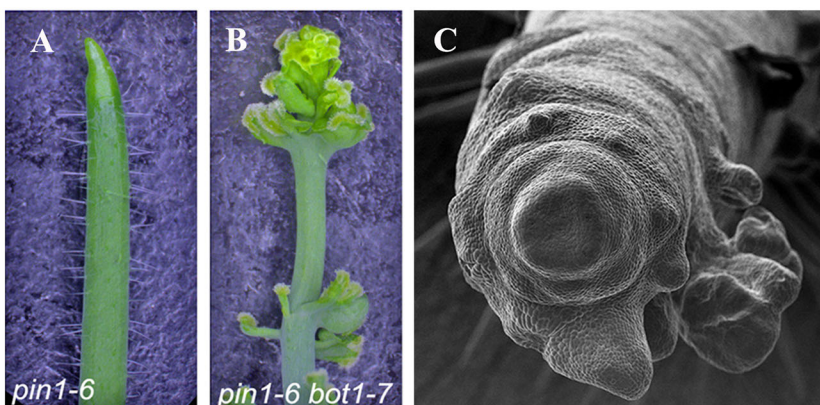

Fig. 1. Restoration of organ formation in a *pin1-6 bot1-7* double mutant. (A) The *pin 1-6* mutant normally forms a naked stem with no or very few lateral organs. (B) This is in contrast to the *pin1-6/bot 1-7* double mutant, which produces many lateral outgrowths. (C) Detailed image of the outgrowths taken with a scanning electron microscope.
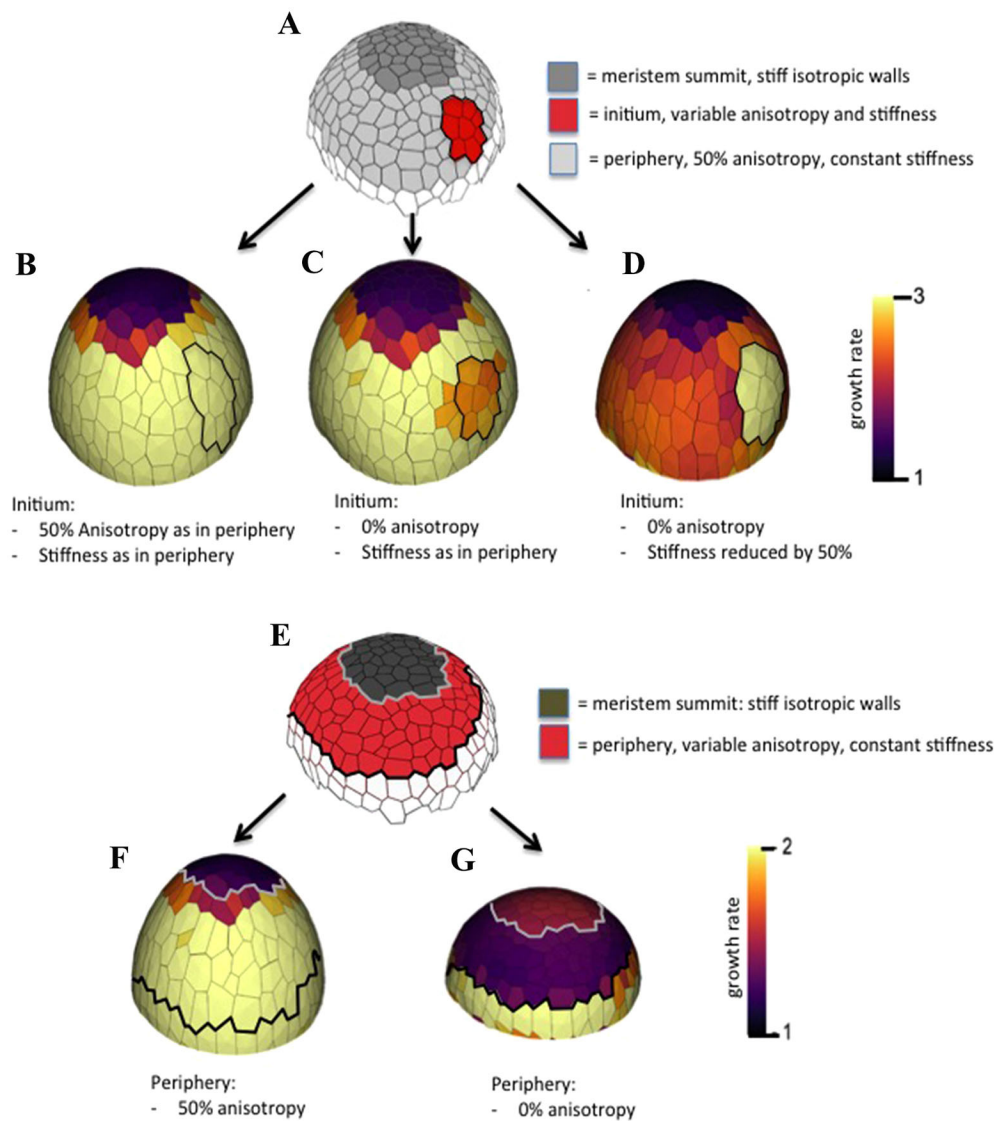
Fig. 2. Influence of mechanical properties on cell expansion: reduced growth rates in isotropic cells. The structure used to perform the various simulations is a 2D shell tiled with polygonal cells. Each cell is composed of several triangular first-order finite elements. The meshes are generated from a segmented 3D confocal stack of images from a *pin* meristem. See Appendix S1 for details. (A,E) The structure at the beginning of the simulations. (B-D,F,G) The structure after 100 steps of growth simulation based on different hypotheses. The relative growth rate is colour coded. In A, a set of initium cells is defined (red zone), which can have variable levels of anisotropy and stiffness. The cells at the summit (dark grey in A and E) are very stiff and grow very slowly. The periphery has a constant stiffness and 50% anisotropy. (B) When the primordium cells have the same stiffness and anisotropy as the peripheral cells, all cells grow at the same rate. (C) When the cells in the primordium are made isotropic, but stiffness remains as in the periphery, the primordium grows more slowly than the surrounding periphery. (D) When both anisotropy and stiffness are reduced, the primordium cells grow quicker than the surrounding cells. In E, the dome has only a peripheral zone with variable mechanical properties. (F) The peripheral cells are anisotropic. (G) When cells are made isotropic, growth rate is reduced.

assumed that the outer cell walls of the meristem are load bearing and rate limiting for growth, whereas the inner cell walls do not significantly contribute to growth control. Arguments come, for example, from electron microscopy data showing that outer wall at the meristem surface is much thicker (Kierzkowski et al., 2012). Experiments using brassinosteroid-deficient mutants also provide evidence that the L1 layer both drives and restricts growth (Savaldi-Goldstein et al., 2007; Hacham et al., 2011). For these reasons, we modelled only the mechanical properties of these outer walls. Recent analyses of turgor pressure in meristematic tissues suggest that the whole meristem behaves as a shell under pressure (Beauzamy et al., 2015). We therefore kept the turgor pressure constant throughout the structure. Growth was implemented through a strain-based law, stating that directional (plastic) expansion of the cell wall is proportional to its elastic stretching minus a given threshold. We assumed the reversible mechanical behaviour of the cell wall to be linear elastic. As elastic strain results from the combination of the elastic properties and turgor-induced mechanical stress, we reasoned that a change from anisotropic to more isotropic microfibril deposition would reduce stiffness in certain directions and increase it in others, leading to directional changes in growth. Considering a growing tissue where microfibril deposition is highly anisotropic, we indirectly changed the growth dynamics of an embedded, small group of cells by making their elastic properties isotropic (see Appendix S1 for further details). Based on the experimental observations, we expected that outer walls with increased isotropy would grow faster than the otherwise highly anisotropic environment. However, simulations following this scenario showed a reduction in growth rate of about 20-25% in a fully isotropic domain surrounded by cells where the degree of anisotropy was 50% (Fig. 2B,C, see Appendix S1 for quantified output). Similarly, even when all the cells at the periphery of the virtual dome were made isotropic, growth rate was reduced by roughly 30% (Fig. 2F,G, see Appendix S1 for quantified output).

Thus, in contrast to experimentation, simulations predicted that isotropy alone is not able to increase cell growth rates. Interestingly, simulations that combined a shift to isotropy with an increase of just 30% in elasticity, which corresponds to the range of measured values in outgrowing organs (Sassi et al., 2014), was sufficient to increase growth rates again (Fig. 2D). This raised the possibility that changes in microtubule orientations would do more than just changing microfibril arrangements and wall anisotropy. We therefore shifted our attention to regulators of cell wall remodelling, in particular those with the potential to modify cell wall mechanics.

DEVELOPMENT

Identification of candidate cell wall remodelling genes involved in organ initiation

A previous study investigating the role of wall synthesis in SAM morphogenesis did not reveal particular changes in the amount of cellulose correlating with organ initiation (Yang et al., 2016; A.A., L.V. and J.T., unpublished). The labelling of cellulose was uneven, but did not show an obvious pattern. In addition, no significant changes in the combined gene activities encoding CESAs were found in outgrowing organs (Yang et al., 2016; A.A., L.V. and J.T., unpublished). We therefore focused our attention on four gene families that have been associated with modifications in the wall matrix: pectin-modifying enzymes (PMEs and PMEIs) and enzymes potentially targeting the hemicellulose matrix and its interactions with cellulose (XTHs and EXPAs).

So far, little is known about the expression patterns of these gene families at the meristem. In a first step, the expression of these cell wall-related genes was investigated by exploiting a RNAseq analysis conducted on dissected inflorescences on which only a minimal segment of stem and the flowers up to stage 2/3 were left.

The results allowed us to identify a set of abundantly expressed candidate genes (Fig. 3A,B; Table S1A-F). Transcripts belonging to all four families were identified in the samples. In particular, genes encoding XTHs were abundantly expressed. Genes encoding PMEIs, PMEs and EXPAs were expressed at a lower level than genes encoding XTHs, but nevertheless more abundantly than the cellulose synthases (Fig. 3A). We next investigated the expression patterns of these genes through in situ hybridization. Of the 31 most abundantly expressed genes tested (see Table S1A-F for a list of tested genes), only 16 were detectable in apical tissues in our hands (see Fig. S1 and Table S1A-F for a complete set of results).

The two most abundantly expressed PMEIs (PMEI AT5G62350 and PMEI3; Fig. 3C; Table S1A-F) were more active in the outgrowing primordia, mainly in the abaxial cell layers of the fast expanding flowers and internodes (Fig. 3C). These zones of high PMEI activity correlated with high labelling of the JIM5 antibody, interacting with partially or entirely de-methyl esterified pectins (Fig. S1, see also Peaucelle et al., 2011a). The third PMEI, AT1G14890, was homogeneously expressed at the meristem.
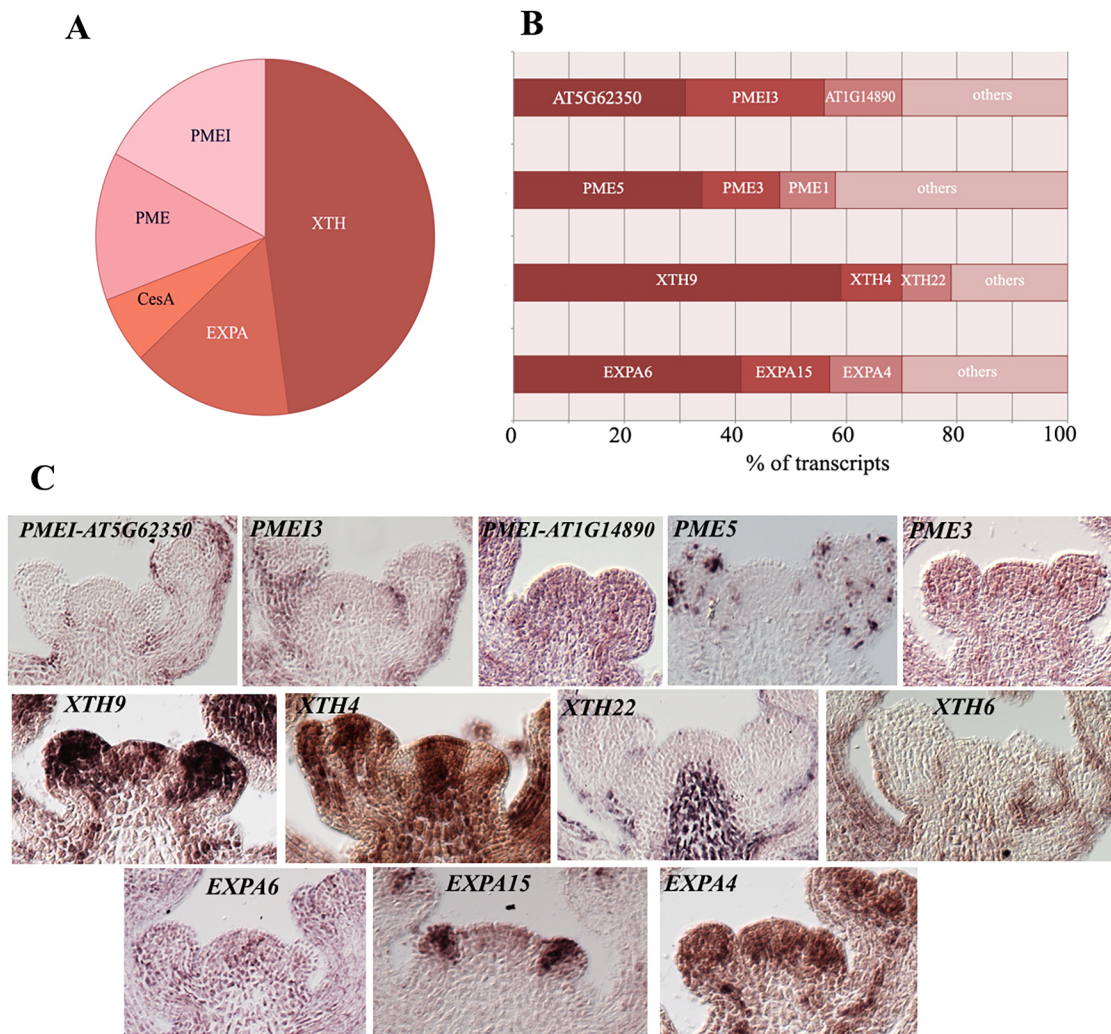

Fig. 3. Expression of putative wall remodelling genes and organ initiation. (A,B) Results from RNAseq of the shoot apex (meristem and young flower primordia). (A) The relative abundance of RNAs encoding XTHs, EXPAs, PMEIs and PMEs compared with CesA. For normalized values taking into account the length of the RNAs, the TPM (transcripts per kilobase million) has been calculated. Note the high relative expression levels of the XTH genes. In B, the relative amounts of the most abundant transcripts within each family are shown. For each family, the three most abundantly expressed genes produce between 58% (PMEs) and 78% (XTHs) of the transcripts of that family. C shows in situ hybridization of the most abundantly expressed RNAs.

PME5 (33% of the PME transcripts) had a spotted expression pattern reminiscent of cell cycle-related genes, as was reported previously (Fig. 3C, see also Peaucelle et al., 2011a). *PME3* (14% of the PME transcripts) was weakly and homogeneously expressed throughout the SAM. RNAs encoding the other PMEs could not be detected.

We next investigated the putative xyloglucan remodelling genes (*XTH* and *EXPA* genes). The RNAseq analysis identified a number of such genes expressed at the shoot apex (see Table S1). *In situ* hybridization confirmed that eight *XTH* and four *EXPA* genes were expressed at the detectable level in apical tissues (Fig. 3C, Fig. S1). Interestingly, three *XTH* genes (*XTH9*, *XTH4* and *XTH22*) and three *EXPA* genes (*EXPA6*, *EXPA15* and *EXPA4*) represented the large majority of the transcripts in each family (Fig. 3A, Table S1A-F). Importantly *XTH9*, *XTH4* and *EXPA15* were expressed at the shoot apex, in particular in the outgrowing flowers. *EXPA15* showed the most restricted pattern, mainly limited to what is the future floral meristem, excluded from the cryptic bract zone. *XTH9* and, in particular, *XTH4* were expressed in the meristem and flower primordia. The expression of XTH9 and, even more obviously, *XTH4* in flower primordia was higher at later developmental stages than in incipient primordia. Two other genes, *EXPA4* and *EXPA6*, were homogenously expressed, whereas *XTH22* was mainly expressed in the vascular tissues and in the differentiating epidermis. Taken together, these data suggest that three genes associated with hemicellulose remodelling (*XTH4*, *XTH9* and *EXPA15*) are highly expressed during the early stages of organ formation.

To check whether these genes are truly correlated with organ emergence, we rescued the naked *pin1*-6 meristem by local applications of auxin. Whereas gene expression could not be detected before treatment, their expression rose as the organ grew out 72-96 h after treatment (Fig. S2). Notably, our RNAseq data did not show any induction of these genes after short auxin treatments (up to 6 h) of the pin-like meristems of plants grown in the presence of the auxin transport inhibitor naphthylphthalamic acid (NPA), suggesting that the effect of auxin on the expression of these genes is largely indirect (results not shown).

Perturbing cortical microtubule organization promotes the expression of wall remodelling genes, independently of auxin accumulation

Our results so far suggested a correlation between microtubule organization, the activation of wall remodelling genes and increased growth rate during organogenesis. Because a change in microtubule organization alone is sufficient to induce outgrowth, we wondered whether this would also induce a change in the expression of the putative wall remodelling genes.

To investigate the existence of such a coupling, we analysed the expression of representatives of the *PME*, *XTH* and *EXPA* families in the *pin1-6 bot1-7* double mutant. In order to obtain a more global view of the expression in the irregularly shaped dome of this mutant, we used whole-mount RNA *in situ* hybridization (Rozier et al., 2014). This showed that *PME3*, *XTH9* and *EXPA15* were highly expressed in the outgrowths (Fig. 4). This result demonstrates that

Fig. 4. Disruption of CMT anisotropy promotes the expression of pectin and xyloglucan modifiers. Expression patterns of *XTH9*, *EXPA15* and *PME3* in *pin1* mutants and *pin1 bot* mutants revealed using whole-mount *in situ* hybridization. Note the upregulation of all three genes in the outgrowths of the double mutant. *PME5* shows a punctuate pattern, probably cell cycle stage specific. Its spotty labelling throughout the meristem is also a control for background noise, which remains low.

these genes can be induced even when auxin transport and distribution are impaired, and suggests that CMT disorganization may contribute to their induction.

In conclusion, the results suggest that the disruption of microtubule alignments indirectly causes the transcriptional activation of three types of wall remodelling genes. The existence of this link between wall isotropy and wall loosening provides a plausible explanation for the increased growth rates induced by the disruption of microtubule organization, and thus matches our simulations combining increased growth isotropy with wall loosening.

We subsequently sought to determine whether the impact of CMT disorganization on outgrowth involves auxin-regulated transcriptional activation. To achieve this, we first examined the transcriptional output marker *DR5::3xVENUS-N7* (Heisler et al., 2005) in a *pin1-6 bot1-7* background. Somewhat surprisingly, this showed that DR5 was activated in this mutant background at highly variable levels. Although even small outgrowths were not necessarily correlated with high DR5 expression (Fig. 5A-C), we could not exclude the possibility that the formation of temporary

auxin peaks in the double mutant were at the basis of these outgrowths. To obtain further information on the dynamics, we monitored the activation of *DR5::3xVENUS-N7* during outgrowth formation in response to local applications of ORY on the SAMs of NPA-grown plantlets. Previous work has shown that this can induce outgrowths that are separated from the meristem by an organ boundary, expressing boundary markers (Landrein et al., 2015). As a control (Fig. 5F) the DR5::3xVENUS-N7 marker displayed a strong activation when organ initiation was induced by locally applied IAA (100%; *n*=10). By contrast, the expression of the DR5::3xVENUS-N7 marker did not change in 24 out of 25 plants when outgrowth was induced by local ORY treatments (Fig. 5G), indicating that perturbing microtubule alignment does not activate auxin signalling within the first 72 h.

Increasing cell wall extensibility promotes the disruption of CMT organization

The results obtained thus far led to a scenario in which auxin would perturb microtubule alignments, which then would (indirectly) feed back on the transcriptional activation of wall-loosening enzymes.
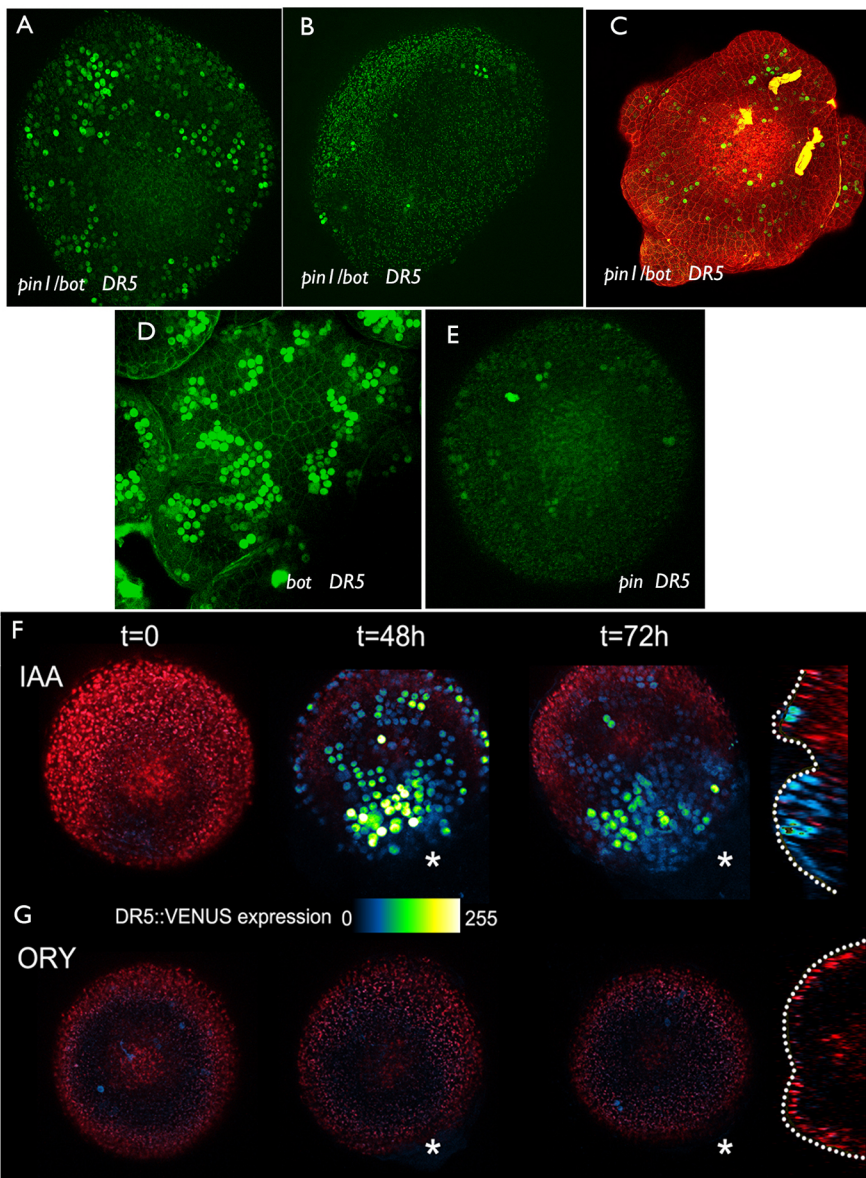

Fig. 5. DR5 activation and outgrowths induced by changed microtubule organization. (A-C) In the *pin bot1* background, DR5 is activated at variable levels, although outgrowth is often not associated with high DR5 levels (C). (D,E) Single *bot* mutants show clear maxima in cell clusters, which can be associated with successive primordia (D), while single *pin* mutants show weak or no DR5 activation (E). (F) When grown on NPA, local auxin treatments systematically activate DR5 expression close to the site of application. (G) Local oryzalin treatment also induces outgrowth (see transverse section on the right), but DR5 is not activated.

This would explain why interfering with microtubule alignments does also lead to increased growth rates and the bulging out of the cells, even when auxin transport is impaired.

Previous studies, however, have shown that interfering with wall properties through the ectopic expression of pectin-modifying enzymes or expansins can also cause outgrowths (Peaucelle et al., 2011a). This made us wonder whether wall loosening induced by pectin or hemicellulose modifiers can also cause changes in microtubule arrangements.

We therefore investigated the effects of perturbing the pectin polymers within the wall using external PME treatment. PMEs in principle reduce wall stiffness by affecting the pectin matrix, and thereby cause the ectopic formation of outgrowths at the SAM. We performed a series of treatments on pin-like meristems formed in the presence of the auxin transport inhibitor NPA. In our hands, all but one of the 22 treated plants showed morphological alterations. Organ formation was observed in seven (31.8%) of the tested SAMs (n=22) (Fig. 6A, Fig. S3). A substantial radial enlargement of the SAM was observed in the majority of the population (14 or 63.6%), with one plant not responding to the treatment (4.5%, see Fig. S3). Regardless of the final effect in all responding meristems, PME treatments affected CMT organization in 35S::GFP-MBD within 48 h (Fig. 6B,C, Fig. S3). In particular, we observed that 24 h after the beginning of the PME treatment most of the meristematic cells still displayed an anisotropic arrangement of CMTs, although in some plants the average CMT orientation shifted from circumferential to longitudinal (Fig. S3). At 48 h after the treatment, the majority of the cells clearly displayed isotropic
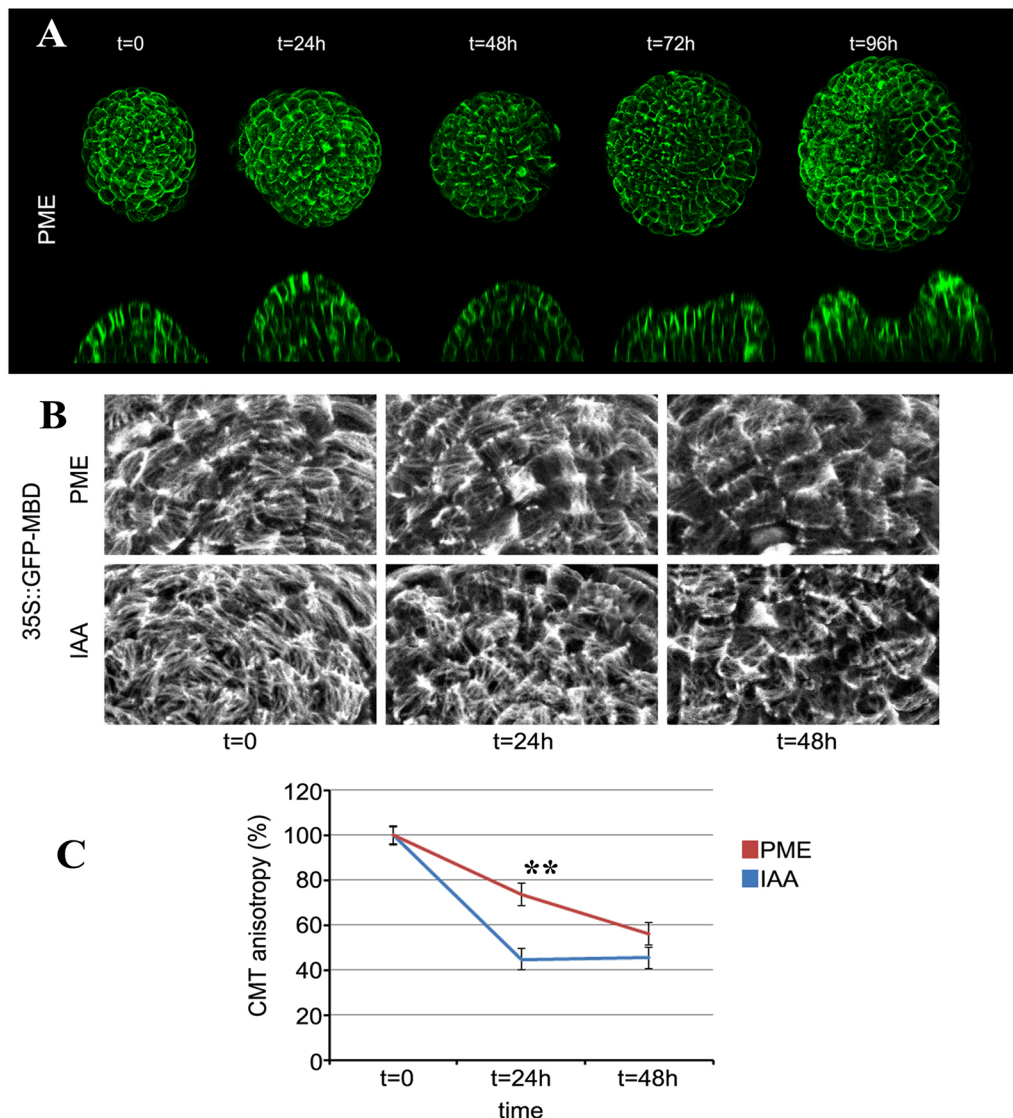

Fig. 6. PME treatment promotes CMT isotropy in SAM cells. (A) PME treatments effect on SAM morphogenesis. NPA-grown plants expressing 35S::MBD: GFP were pictured before (t=0) and up to 96 h after the beginning of the PME treatment. Top views (upper row) and longitudinal sections (bottom row) are shown of a meristem forming a ring-like outgrowth. (B,C) PME treatments promote long-term disruption of CMT organization in SAM cells. (B) Details of SAM cells of NPA-grown 35S::GFP-MBD treated with PME (top row) and IAA (bottom row). (C) Relative quantification of CMT isotropy in SAM cells grown as in B. In both cases, the treatment leads to a reduction in anisotropy. At least 140 cells were measured in three plants for each condition. The level of anisotropy in every cell was calculated using the Fiji plug-in 'fibril tool'. Error bars represent s.e.m. Statistical analysis (t-test) of data in C showed that: in PME-treated plants, the degree of anisotropy is already significantly lower at 24 h than at the beginning of the treatment treatment (**P<0.01); and in IAA-treated plants, the degree of anisotropy is significantly lower at 24 h than at the beginning of the treatment (**P<0.01). Only at 24 h is there also a significant difference between IAA and PME treatments (**P<0.01).

CMT arrangements. It must be pointed out that the disruption of CMT organization by PME is substantially slower and less abrupt compared with that induced by IAA in control experiments. Indeed, only at 24 h the values of PME- and IAA-treated plants are significantly different at 24 h ($P<0.01$).

We next tested whether perturbing wall remodelling genes potentially targeting the hemicellulose matrix would also affect microtubules and cause the formation of outgrowths in the absence of auxin transport. Unfortunately, single and double *xth4* and *xth9* (Fig. S4) mutants, as well as *expa15* knockouts (not shown, see Materials and Methods) did not show any obvious phenotype. We therefore focused our attention on the *xxt1 xxt2* double mutant. The *XXT1* and *XXT2* genes encode XG xylosyl-transferases, which are both expressed at the shoot apex (Yang et al., 2016). Mutants lacking both genes have very little or no xyloglucans, and have retarded growth and reduced gravitropism. They are nevertheless able to produce lateral organs such as branches, leaves and flowers (Fig. S4, see also Park and Cosgrove, 2012a; Cavalier et al., 2008).

On NPA treatment, a particular phenotype was observed. In our hands, 60% ($n=265$) of wild-type plants grown on NPA form pin-like stems, while 38% occasionally formed one or more lateral flowers or floral organs. This is at least partially because the microtubules maintain a highly anisotropic organization, thus promoting the formation of a cylindrical stem. Interestingly, when grown on NPA, 32% ($n=212$) of the *xxt1 xxt2* mutants showed the formation of multiple spontaneous outgrowths (Fig. 7A-J) never seen in wild-type plants. Wild-type plants occasionally formed the same type of outgrowths (2%), but never that many per apex. A double mutant line expressing *MBD::GFP* in the L1 layer of the meristem showed that this phenotype on NPA went along with altered microtubule organization. In particular, the zone of isotropic microtubule arrays at the meristem summit was extended to a variable degree (Fig. 7D-I). Outside this zone, the cells were able to align their microtubules circumferentially around the stem. This implies that the level of xyloglucans can influence microtubule alignment at the shoot apex. However, this only leads to a clear phenotype and ectopic outgrowth in the absence of auxin accumulation, when auxin transport is perturbed.

DISCUSSION

Shape changes during morphogenesis in plants are achieved through the local isotropic or anisotropic yielding of the cell wall to the
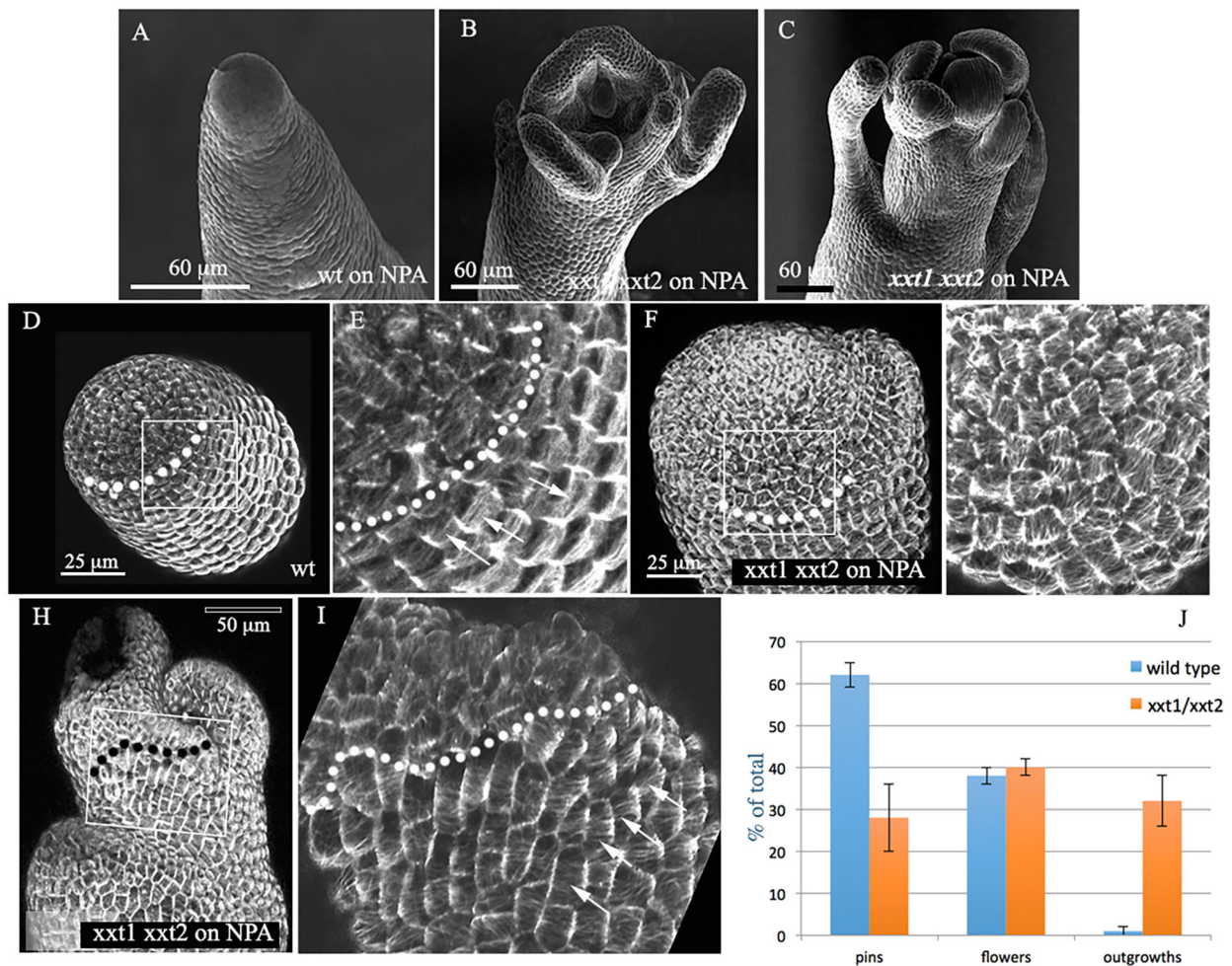

Fig. 7. Effect of *xxt1 xxt2* double mutation on organ production. (A-C) SEM images depicting the SAM phenotypes of the *xxt1 xxt2* double mutant grown on NPA compared with the wild type (Col-0). (D,E) Overview (D) and detail (E) of a wild-type meristem expressing MBD:GFP grown on NPA. The dotted line indicates the limit between the isotropic microtubules (arrows in E) at the dome and the anisotropic beginning of the stem. (F-I) Two examples of the *xxt1 xxt2* mutant. In both cases, the isotropic zone is extended (limits indicated by dotted lines), which is correlated with the formation of lateral outgrowths. The cells are able to align their microtubules lower down (arrows in I). (J) Quantification of phenotypes (%) in wild type and mutants on NPA, based on three independent series of plants for each genotype (data are mean±s.d.). Sixty-two percent of the wild-type plants ($n=265$) formed naked pins, 38% formed one or more flowers, while 2% formed a limited number of non-defined outgrowths. In the mutant, 32% of the total number of plants ($n=212$) produced multiple outgrowths.

internal turgor pressure. In a previous study, we highlighted the regulation of structural wall anisotropy during organ initiation at the shoot apical meristem (Sassi et al., 2014). The local accumulation of auxin destabilizes microtubule alignment, probably via a ROP-based signalling cascade. This supposedly causes a shift to isotropic microfibril deposition and consequently to isotropic growth and the formation of a new growth axis. Intuitively it seemed plausible that a group of structurally isotropic cells in an anisotropic environment would spontaneously bulge out. Our numerical simulations, however, predicted that this is not sufficient, and can even go against outgrowth. Indeed, structurally isotropic walls expand more slowly than anisotropic walls in the simulations if all other mechanical parameters are kept identical. This is probably because cell wall stiffness in a particular direction is not a linear function of the number of microfibrils in that direction. Fibrils aligned in other similar directions also contribute, generating a cooperative effect with a counter-intuitive consequence: when the structural anisotropy of the cell wall evolves, the average rigidity changes, although the number of fibrils remains constant. This change in wall stiffness in turn also affects growth rates (see Appendix S1 for detailed explanations). In our simulations this property led to decreased growth rates when the outer walls were made more isotropic.

Coupling anisotropy to wall loosening

The simulations left us with a contradiction: *in vivo*, mechanical isotropy of the walls seemed to be synonymous with increased growth rates and organ formation, whereas simulations predicted that the exact opposite should happen. We resolved this apparent contradiction by showing that, in contrast to the simulations, where rigidity and anisotropy can be programmed independently, we were so far not able to separate both parameters experimentally. This can be explained because a shift to isotropic growth *in vivo* also triggers an increase in the expression of wall-loosening proteins. At this stage, it remains unclear how this transcriptional coupling functions, as cell wall loosening likely depends on many inputs. Changes in microtubule dynamics could even lead, for example, to problems with membrane trafficking and exocytosis of wall-modelling enzymes. It is also possible that a shift to isotropic deposition of cellulose microfibrils, is sensed by receptors at the cell surface. In this context, it is important to note that isoxaben treatment, which affects cellulose synthesis and cell expansion led to the activation of EXPA15 (A.A.R and J.T., unpublished). Another important issue concerns the transcription factors that actually activate cell wall-loosening enzymes and whether this can also occur via auxin-independent pathways.

Whatever the molecular basis, the coupling between wall loosening and isotropy could provide a mechanical module that is essential for establishing the typical branched plant architecture. It remains to be seen if and how this coupling functions in other developmental contexts. It seems, for example, to be inactive in slow-growing cells of the meristem centre, where microtubules are fully isotropic and the wall-loosening genes identified are not activated. However, it could be widely activated in other parts of the growing plant. A previous study identified a regulatory cross-talk between microtubules and XTHs, which control petiole elongation in shaded plants downstream of auxin action (Sasidharan et al., 2014). Moreover, a recent cellular analysis of the *xxt1 xxt2* mutant exhibited a loss of microtubule alignment in hypocotyls (Xiao et al., 2016). It was also found that the expression of several microtubule-associated genes, including MAP70-5 and CLASP, as well as receptor genes such as *HERK1* and *WAK1*, were changed in *xxt1 xxt2* mutants (Xiao et al., 2016). Together, these results indicate that a transcriptional coupling between xyloglucan loosening and CMT

organization is not restricted to the SAM but could be involved in the regulation of different developmental processes.

Organ initiation and the wall matrix

A recent comprehensive analysis showed that the enzymes involved in hemicellulose synthesis play an important role throughout the meristematic apex (Xiao et al., 2014). Our finding that several *XTH* and *EXPA* genes are very strongly expressed in outgrowing organs would suggest a prominent role for xyloglucan modifications, in line with the results of previous studies on organogenesis in tomato (Fleming et al., 1997; Reinhardt et al., 1998). Although double mutants where *XTH4* was knocked out and *XTH9* was almost completely suppressed have reduced XET activity in the stems (E.M., A. Banasiak, N. Nishikubo, S. Kushwah, S. Philippe, M. Majda, M. Derba-Maceluch, V. Kumar, A. Gorzsas, S. Endo, B. Sundberg and J. Braam, unpublished), these mutants did not show strong phenotypes under normal conditions. Likewise, an *expa15* knockout did not show any obvious effect (not shown). This probably reflects the extraordinary flexibility of the cell wall assembly and remodelling network. Nevertheless, the *xxt1 xxt2* mutant produced lateral outgrowths when auxin transport was inhibited, showing that the control of xyloglucan synthesis is at least partially responsible for the pin phenotype.

Several studies have also pointed at the importance of pectins in morphogenesis at the shoot apex (Peaucelle et al., 2011a,b, 2008). However, Yang and colleagues did not find obvious differences in the degree of pectin methylation related to organ initiation at the SAM (Yang et al., 2016). We confirmed these results and found that PMEIs are much more strongly expressed in the more differentiating, expanding cells on the abaxial side of the organ primordia. This is surprising, at least at first sight, because this is in apparent contradiction with a higher level of de-methyl esterified pectins at the same domain when detected using immunolabelling. At this stage, it is difficult to provide an explanation, in particular because the precise enzymatic activity of the esterases and their inhibitors at the meristem remains to be established. However the expression of PMEs, PMEIs and the level of de-methyl esterified pectin seems to be rather homogeneous at the meristem proper (see also Krizek et al., 2016). Our analysis therefore leads to a hypothesis where the degree of pectin methylation is not subject to major changes during the very early stages of organ initiation. This does imply, however, that pectin homeostasis would need to be regulated in a strict manner at the meristem. Accordingly, modifications perturbing this homeostasis through overexpression of PMEs or PMEIs lead to extra outgrowth or to the inhibition of organ initiation, respectively (Peaucelle et al., 2008).

Conclusions and perspectives

In conclusion, we provide evidence for the existence of a mechanical module at the shoot apex, which couples the transcriptional regulation of wall expansion to cellular mechanical anisotropy. This module coordinates changes in growth rates and growth directions to drive the formation of new organs. An important challenge will be to further unravel the coupling mechanisms and what signalling components and transcription factors are involved. More generally, it will be important to investigate how this coordination between wall loosening and anisotropy is modulated throughout plant development.

MATERIALS AND METHODS
Plant material, growth conditions and chemical treatments
Arabidopsis thaliana plants of the ecotypes Columbia-0 (Col-0) and Wassilewskija-2 (Ws-2) were used as wild type.

DEVELOPMENT

Transgenic lines and some of the mutants used in this study have been previously described: plants expressing the membrane marker 35S::LTi6b-GFP (Cutler et al., 2000), *pin1-6* and *bot1-7 pin1-6* (Sassi et al., 2014), and *xxt1 xxt2* (Cavalier et al., 2008).

The xth4 and xth9 mutants were obtained as single T-DNA insertion lines SAIL_681_G09 and SAIL_722_B10 after backcrossing (E.M, A. Banasiak, N. Nishikubo, S. Kushwah, S. Philippe, M. Majda, M. Derba-Maceluch, V. Kumar, A. Gorzsas, S. Endo, B. Sundberg and J. Braam, unpublished). Plants were grown as previously described (Sassi et al., 2014).

To generate the PDF1::mCitrine-MBD plasmids, the MultiSite Gateway Three-Fragment strategy (Life Technologies) was used: a 1456 pb promoter sequence upstream of PDF1 (Landrein et al., 2015), the fluorophore mCitrine and the MBD domains (Marc et al., 1998) were cloned in pDONR-P4P1R, pDONR-221 and pDONR-P2RP3 vectors, respectively, and inserted in pBART (basta resistant) as a destination vector. Col-0 plants were transformed by dipping inflorescences as described by Simon et al. (2016). Naphthylphthalamic acid (NPA), indole-3-acetic acid (IAA) and oryzalin (ORY) treatments were carried out as previously described.

A Ds insertion line in the second exon, T-DNA of the *EXPA15* gene (ET6476.DS3.07.21.98.B.75, ARBC Stock Center), in the Ler background had a barely detectable expression level, but did not show any visible phenotype.

Treatments with PME (Pectinesterase, from Orange peel P5400-1KU 065K7435 Sigma-Aldrich) were carried out as previously described (Peaucelle et al., 2008), with some modifications: plants were grown *in vitro* on NPA-treated plates until bolting, then they were transferred onto fresh NPA-treated plates and imaged (t=0). Immediately after imaging, plants were submerged in a PME solution [1 U/100 µl in 50 mM phosphate buffer (pH=7)] for 16 h. Plants were imaged again at t=24 h, and the treatment was repeated immediately after. No further treatments were applied until the end of the experiment.

Confocal live imaging and image analyses

Confocal imaging was carried out on a Zeiss LSM700 system as previously described (Sassi et al., 2014). SEM imaging was carried out on a Hirox SE-3000 system as previously described (Sassi et al., 2014). Analyses of CMT organization were carried out with FIJI software as previously described (Sassi et al., 2014). Microtubule anisotropy was calculated for every cell using the fibril tool. This is an ImageJ plug-in based on the concept of a nematic tensor, which can provide a quantitative description of the anisotropy of fibre arrays and their average orientation in cells, directly from raw images obtained by any form of microscopy (Boudaoud et al., 2014).

RNAseq sample preparation and sequencing analysis

Ten dissected (to P5) Col-0 meristems were pooled for each biological replicate. RNA was extracted using the Arcturus PicoPure RNA extraction kit (ThermoFisher) according to the manufacturer's instructions. Libraries were prepared using the TruSeq Strand-specific protocol following manufacturer's instructions. The three RNAseq libraries were sequenced using a HiSeq2000 Pair End 2×100 bp at the Unité de Recherche en Génomique Végétale (Institute of Plant Sciences Paris-Saclay). The raw reads in fastq format were analysed in house. We first assessed the quality of the reads using FastQC (http://www.bioinformatics.babraham.ac.uk/projects/fastqc). Reads were cleaned (quality threshold: 20, adaptors removed, and reads mapping to rRNA removed). Preprocessed reads were then mapped to the Col-0 reference genome using Bowtie 2 and TopHat and counted using HTSeq. TPM (transcripts per million kilobases) were calculated for each gene by dividing the raw number of reads to the length of the cDNA in kb, normalized to the number of reads per biological replicate in million reads. All raw and normalized data are available in GEO (GSE114862) (Barrett et al., 2007).

Histochemistry

RNA *in situ* hybridization assays were performed as described previously (Ferrandiz and Sessions, 2008a,b). For whole-mount RNA *in situ* hybridization assays, untreated and treated (IAA or ORY) *pin1-6* meristems from soil-grown plants were processed as previously described

(Rozier et al., 2014). At least three independent experiments for both assays were performed for each probe tested. Whole-mount immunolabellings were carried out as previously described. Cell wall antibodies were obtained from the Plant Probes service at the University of Leeds, UK (http://www.plantprobes.net/index.php).

Quantitative reverse transcription PCR (qRT-PCR)

Total RNA was extracted using the Spectrum Plant Total RNA Kit (Sigma). Total RNAs were digested on-column with Turbo DNA-free DNase I (Ambion) according to the manufacturer's instructions. SuperScript VILO cDNA Synthesis Kit (Invitrogen) was used to reverse transcribe RNA. The quantitative reverse transcription PCR (qRT-PCR) was performed on a StepOne Plus Real Time PCR System (Applied Biosystems), using FastStart Universal SYBR Green Master (Rox) (Roche). Data were analysed using the StepOne Software v2.2 (Applied Biosystems). TCTP gene has been used as reference. Expression levels of each target gene, relative to TCTP, were determined using a modification of the Pfaffl method (Pfaffl, 2001). Primers are listed in Table S2.

References
Barrett, T., Troup, D. B., Wilhite, S. E., Ledoux, P., Rudnev, D., Evangelista, C., Kim, I. F., Soboleva, A., Tomashevsky, M. and Edgar, R. (2007). NCBI GEO: mining tens of millions of expression profiles–database and tools update. *Nucleic Acids Res.* **35**, D760-D765.

Beauzamy, L., Louveaux, M., Hamant, O. and Boudaoud, A. (2015). Mechanically, the shoot apical meristem of arabidopsis behaves like a shell inflated by a pressure of about 1 MPa. *Front. Plant Sci.* **6**, 1038.

Boudaoud, A., Burian, A., Borowska-Wykręt, D., Uyttewaal, M., Wrzalik, R., Kwiatkowska, D. and Hamant, O. (2014). FibrilTool, an ImageJ plug-in to quantify fibrillar structures in raw microscopy images. *Nat. Protoc.* **9**, 457-463.

Boudon, F., Chopard, J., Ali, O., Gilles, B., Hamant, O., Boudaoud, A., Traas, J. and Godin, C. (2015). A computational framework for 3D mechanical modeling of plant morphogenesis with cellular resolution. *PLoS Comput. Biol.* **11**, e1003950.

Braybrook, S. A. and Jönsson, H. (2016). Shifting foundations: the mechanical cell wall and development. *Curr. Opin. Plant Biol.* **29**, 115-120.

Cavalier, D. M., Lerouxel, O., Neumetzler, L., Yamauchi, K., Reinecke, A., Freshour, G., Zabotina, O. A., Hahn, M. G., Burgert, I., Pauly, M. et al. (2008). Disrupting two Arabidopsis thaliana xylosyltransferase genes results in plants deficient in xyloglucan, a major primary cell wall component. *Plant Cell* **20**, 1519-1537.

Coen, E., Rolland-Lagan, A. G., Matthews, M., Bangham, J. A. and Prusinkiewicz, P. (2004). The genetics of geometry. *Proc. Natl. Acad. Sci. USA* **101**, 4728-4735.

Cosgrove, D. J. (2015). Plant expansins: diversity and interactions with plant cell walls. *Curr. Opin. Plant Biol.* **25**, 162-172.

DEVELOPMENT

Cosgrove, D. J. (2016a). Catalysts of plant cell wall loosening. *F1000Res* **5**, 119.

Cosgrove, D. J. (2016b). Plant cell wall extensibility: connecting plant cell growth with cell wall structure, mechanics, and the action of wall-modifying enzymes. *J. Exp. Bot.* **67**, 463-476.

Cutler, S. R., Ehrhardt, D. W., Griffitts, J. S. and Somerville, C. R. (2000). Random GFP::cDNA fusions enable visualization of subcellular structures in cells of Arabidopsis at a high frequency. *Proc. Natl. Acad. Sci. USA* **97**, 3718-3723.

Ferrandiz, C. and Sessions, A. (2008a). Nonradioactive in situ hybridization of RNA probes to sections of plant tissues. *CSH Protoc* **2008**, pdb prot4943.

Ferrandiz, C. and Sessions, A. (2008b). Preparation and hydrolysis of digoxygenin-labeled probes for in situ hybridization of plant tissues. *CSH Protoc* **2008**, pdb prot4942.

Fleming, A. J., Mcqueenmason, S., Mandel, T. and Kuhlemeier, C. (1997). Induction of leaf primordia by the cell wall protein expansin. *Science* **276**, 1415-1418.

Gilmour, D., Rembold, M. and Leptin, M. (2017). From morphogen to morphogenesis and back. *Nature* **541**, 311-320.

Hacham, Y., Holland, N., Butterfield, C., Ubeda-Tomas, S., Bennett, M. J., Chory, J. and Savaldi-Goldstein, S. (2011). Brassinosteroid perception in the epidermis controls root meristem size. *Development* **138**, 839-848.

Heisler, M. G., Ohno, C., Das, P., Sieber, P., Reddy, G. V., Long, J. A. and Meyerowitz, E. M. (2005). Patterns of auxin transport and gene expression during primordium development revealed by live imaging of the Arabidopsis inflorescence meristem. *Curr. Biol.* **15**, 1899-1911.

Kierzkowski, D., Nakayama, N., Routier-Kierzkowska, A.-L., Weber, A., Bayer, E., Schorderet, M., Reinhardt, D., Kuhlemeier, C. and Smith, R. S. (2012). Elastic domains regulate growth and organogenesis in the plant shoot apical meristem. *Science* **335**, 1096-1099.

Krizek, B. A., Bequette, C. J., Xu, K., Blakley, I. C., Fu, Z. Q., Stratmann, J. W. and Loraine, A. E. (2016). RNA-Seq links the transcription factors AINTEGUMENTA and AINTEGUMENTA-LIKE6 to cell wall remodeling and plant defense pathways. *Plant Physiol.* **171**, 2069-2084.

Kwiatkowska, D. (2004). Surface growth at the reproductive shoot apex of Arabidopsis thaliana pin-formed 1 and wild type. *J. Exp. Bot.* **55**, 1021-1032.

Kwiatkowska, D. and Dumais, J. (2003). Growth and morphogenesis at the vegetative shoot apex of Anagallis arvensis L. *J. Exp. Bot.* **54**, 1585-1595.

Landrein, B., Kiss, A., Sassi, M., Chauvet, A., Das, P., Cortizo, M., Laufs, P., Takeda, S., Aida, M., Traas, J. et al. (2015). Mechanical stress contributes to the expression of the STM homeobox gene in Arabidopsis shoot meristems. *Elife* **4**, e07811.

Levesque-Tremblay, G., Pelloux, J., Braybrook, S. A. and Müller, K. (2015). Tuning of pectin methylesterification: consequences for cell wall biomechanics and development. *Planta* **242**, 791-811.

Lin, D., Cao, L., Zhou, Z., Zhu, L., Ehrhardt, D., Yang, Z. and Fu, Y. (2013). Rho GTPase signaling activates microtubule severing to promote microtubule ordering in Arabidopsis. *Curr. Biol.* **23**, 290-297.

Marc, J., Granger, C. L., Brincat, J., Fisher, D. D., Kao, T., Mccubbin, A. G. and Cyr, R. J. (1998). A GFP-MAP4 reporter gene for visualizing cortical microtubule rearrangements in living epidermal cells. *Plant Cell* **10**, 1927-1940.

Nishitani, K. V. (2006). Roles of the XTH protein family in the expanding cell. *Plant Cell Monographs* **5**, 89-116.

Paredez, A. R., Somerville, C. R. and Ehrhardt, D. W. (2006). Visualization of cellulose synthase demonstrates functional association with microtubules. *Science* **312**, 1491-1495.

Park, Y. B. and Cosgrove, D. J. (2012a). Changes in cell wall biomechanical properties in the xyloglucan-deficient xxt1/xxt2 mutant of Arabidopsis. *Plant Physiol.* **158**, 465-475.

Park, Y. B. and Cosgrove, D. J. (2012b). A revised architecture of primary cell walls based on biomechanical changes induced by substrate-specific endoglucanases. *Plant Physiol.* **158**, 1933-1943.

Peaucelle, A., Louvet, R., Johansen, J. N., Hofte, H., Laufs, P., Pelloux, J. and Mouille, G. (2008). Arabidopsis phyllotaxis is controlled by the methyl-esterification status of cell-wall pectins. *Curr. Biol.* **18**, 1943-1948.

Peaucelle, A., Braybrook, S. A., Le Guillou, L., Bron, E., Kuhlemeier, C. and Hofte, H. (2011a). Pectin-induced changes in cell wall mechanics underlie organ initiation in Arabidopsis. *Curr. Biol.* **21**, 1720-1726.

Peaucelle, A., Louvet, R., Johansen, J. N., Salsac, F., Morin, H., Fournet, F., Belcram, K., Gillet, F., Hofte, H., Laufs, P. et al. (2011b). The transcription factor BELLRINGER modulates phyllotaxis by regulating the expression of a pectin methylesterase in Arabidopsis. *Development* **138**, 4733-4741.

Peaucelle, A., Wightman, R. and Hofte, H. (2015). The control of growth symmetry breaking in the arabidopsis hypocotyl. *Curr. Biol.* **25**, 1746-1752.

Pfaffl, M. W. (2001). A new mathematical model for relative quantification in real-time RT-PCR. *Nucleic Acids Res.* **29**, e45.

Reinhardt, D., Wittwer, F., Mandel, T. and Kuhlemeier, C. (1998). Localized upregulation of a new expansin gene predicts the site of leaf formation in the tomato meristem. *Plant Cell* **10**, 1427-1437.

Reinhardt, D., Mandel, T. and Kuhlemeier, C. (2000). Auxin regulates the initiation and radial position of plant lateral organs. *Plant Cell* **12**, 507-518.

Reinhardt, D., Pesce, E. R., Stieger, P., Mandel, T., Baltensperger, K., Bennett, M., Traas, J., Friml, J. and Kuhlemeier, C. (2003). Regulation of phyllotaxis by polar auxin transport. *Nature* **426**, 255-260.

Rose, J. K., Braam, J., Fry, S. C. and Nishitani, K. (2002). The XTH family of enzymes involved in xyloglucan endotransglucosylation and endohydrolysis: current perspectives and a new unifying nomenclature. *Plant Cell Physiol.* **43**, 1421-1435.

Rozier, F., Mirabet, V., Vernoux, T. and Das, P. (2014). Analysis of 3D gene expression patterns in plants using whole-mount RNA in situ hybridization. *Nat. Protoc.* **9**, 2464-2475.

Sasidharan, R., Keuskamp, D. H., Kooke, R., Voesenek, L. A. C. J. and Pierik, R. (2014). Interactions between auxin, microtubules and XTHs mediate green shade- induced petiole elongation in arabidopsis. *PLoS ONE* **9**, e90587.

Sassi, M. and Traas, J. (2015). When biochemistry meets mechanics: a systems view of growth control in plants. *Curr. Opin. Plant Biol.* **28**, 137-143.

Sassi, M., Ali, O., Boudon, F., Cloarec, G., Abad, U., Cellier, C., Chen, X., Gilles, B., Milani, P., Friml, J. et al. (2014). An auxin-mediated shift toward growth isotropy promotes organ formation at the shoot meristem in Arabidopsis. *Curr. Biol.* **24**, 2335-2342.

Savaldi-Goldstein, S., Peto, C. and Chory, J. (2007). The epidermis both drives and restricts plant shoot growth. *Nature* **446**, 199-202.

Simon, M. L., Platre, M. P., Marques-Bueno, M. M., Armengot, L., Stanislas, T., Bayle, V., Caillaud, M.-C. and Jaillais, Y. (2016). A PtdIns(4)P-driven electrostatic field controls cell membrane identity and signalling in plants. *Nat. Plants* **2**, 16089.

Traas, J. and Hamant, O. (2009). From genes to shape: understanding the control of morphogenesis at the shoot meristem in higher plants using systems biology. *C. R. Biol.* **332**, 974-985.

Xiao, C., Somerville, C. and Anderson, C. T. (2014). POLYGALACTURONASE INVOLVED IN EXPANSION1 functions in cell elongation and flower development in Arabidopsis. *Plant Cell* **26**, 1018-1035.

Xiao, C., Zhang, T., Zheng, Y., Cosgrove, D. J. and Anderson, C. T. (2016). Xyloglucan deficiency disrupts microtubule stability and cellulose biosynthesis in arabidopsis, altering cell growth and morphogenesis. *Plant Physiol.* **170**, 234-249.

Yang, W., Schuster, C., Beahan, C. T., Charoensawan, V., Peaucelle, A., Bacic, A., Doblin, M. S., Wightman, R. and Meyerowitz, E. M. (2016). Regulation of meristem morphogenesis by cell wall synthases in arabidopsis. *Curr. Biol.* **26**, 1404-1415.